Checkpoint Receptor TIGIT Expressed on Tim-1+ B Cells Regulates Tissue Inflammation

Xiao, Sheng ; Bod, Lloyd ; Pochet, Nathalie ; Kota, Savithri Balasubramanian ; Hu, Dan ; Madi, Asaf ; Kilpatrick, Jessica ; Shi, Jingwen ; Ho, Allen ; Zhang, Huiyuan ; Sobel, Raymond ; Weiner, Howard L ; Strom, Terry B ; Quintana, Francisco J ; Joller, Nicole ; Kuchroo, Vijay K

Abstract: Tim-1, a phosphatidylserine receptor expressed on B cells, induces interleukin 10 (IL-10) production by sensing apoptotic cells. Here we show that mice with B cell-specific Tim-1 deletion develop tissue inflammation in multiple organs including spontaneous paralysis with inflammation in the central nervous system (CNS). Transcriptomic analysis demonstrates that besides IL-10, Tim-1+ B cells also differentially express a number of co-inhibitory checkpoint receptors including TIGIT. Mice with B cell-specific TIGIT deletion develop spontaneous paralysis with CNS inflammation, but with limited inflammation in other organs. Our findings suggest that Tim-1+ B cells are essential for maintaining self-tolerance and restraining tissue inflammation, and that Tim-1 signaling-dependent TIGIT expression on B cells is essential for maintaining CNS-specific tolerance. A possible critical role of aryl hydrocarbon receptor (AhR) in regulating the B cell function is discussed, as we find that AhR is among the preferentially expressed transcription factors in Tim-1+ B cells and regulates their TIGIT and IL-10 expression.

DOI: https://doi.org/10.1016/j.celrep.2020.107892

Cell Reports

Checkpoint Receptor TIGIT Expressed on Tim-1^{+} B Cells Regulates Tissue Inflammation

Graphical Abstract

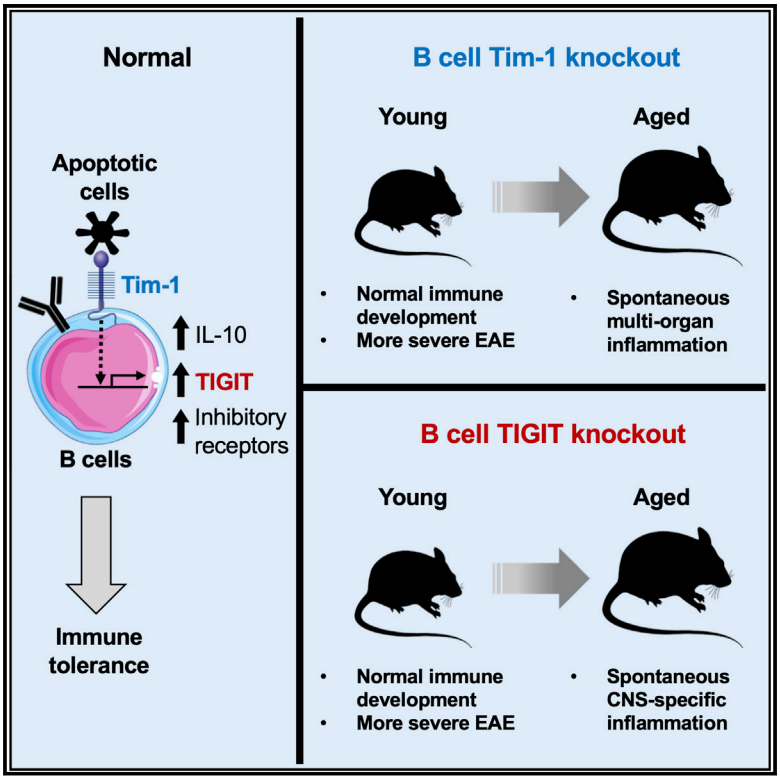

Highlights

- Tim-1^{+} B cells are required for maintaining immune tolerance
- Tim-1^{+} B cells differentially express TIGIT and other co-inhibitory molecules
- B cell expression of TIGIT and many other regulators requires Tim-1 signaling
- B cell TIGIT expression is preferentially required for maintaining CNS tolerance

Authors

Sheng Xiao, Lloyd Bod, Nathalie Pochet, ..., Francisco J. Quintana, Nicole Joller, Vijay K. Kuchroo

Correspondence

sxiao@celsiustx.com (S.X.), vkuchroo@evergrande.hms.harvard.edu (V.K.K.)

In Brief

Xiao et al. find that Tim-1 expression and signaling in B cells is required for maintaining self-tolerance. Tim-1^{+} B cells execute their regulatory function by expressing a set of negative immune regulators, of which checkpoint receptor TIGIT is preferentially required for the B cell-mediated tolerance in the central nervous system.

Xiao et al., 2020, Cell Reports *32*, 107892
July 14, 2020
https://doi.org/10.1016/j.celrep.2020.107892

CellPress

Cell Reports

CellPress
OPEN ACCESS

Report

Checkpoint Receptor TIGIT Expressed on Tim-1$^+$ B Cells Regulates Tissue Inflammation

Sheng Xiao,[1,6,*] Lloyd Bod,[1] Nathalie Pochet,[1,8] Savithri Balasubramanian Kota,[2,8] Dan Hu,[1] Asaf Madi,[1,7] Jessica Kilpatrick,[1] Jingwen Shi,[1] Allen Ho,[1] Huiyuan Zhang,[1] Raymond Sobel,[3] Howard L. Weiner,[1] Terry B. Strom,[4] Francisco J. Quintana,[1] Nicole Joller,[5] and Vijay K. Kuchroo[1,9,*]

[1]Evergrande Center for Immunologic Diseases and Ann Romney Center for Neurologic Diseases, Harvard Medical School and Brigham and Women's Hospital, Boston, MA 02115, USA
[2]Renal Division, Beth Israel Deaconess Medical Center and Harvard Medical School, Boston, MA 02115, USA
[3]Palo Alto Veteran's Administration Health Care System and Department of Pathology, Stanford University School of Medicine, Stanford, CA, USA
[4]Transplant Institute, Beth Israel Deaconess Medical Center and Harvard Medical School, Boston, MA 02115, USA
[5]Institute of Experimental Immunology, University of Zurich, Zurich 8057, Switzerland
[6]Present address: Celsius Therapeutics, Cambridge, MA 02139, USA
[7]Present address: Department of Pathology, Sackler School of Medicine, Tel Aviv University, Tel Aviv, Israel
[8]These authors contributed equally
[9]Lead Contact
*Correspondence: sxiao@celsiustx.com (S.X.), vkuchroo@evergrande.hms.harvard.edu (V.K.K.)
https://doi.org/10.1016/j.celrep.2020.107892

SUMMARY

Tim-1, a phosphatidylserine receptor expressed on B cells, induces interleukin 10 (IL-10) production by sensing apoptotic cells. Here we show that mice with B cell-specific Tim-1 deletion develop tissue inflammation in multiple organs including spontaneous paralysis with inflammation in the central nervous system (CNS). Transcriptomic analysis demonstrates that besides IL-10, Tim-1$^+$ B cells also differentially express a number of co-inhibitory checkpoint receptors including TIGIT. Mice with B cell-specific TIGIT deletion develop spontaneous paralysis with CNS inflammation, but with limited inflammation in other organs. Our findings suggest that Tim-1$^+$ B cells are essential for maintaining self-tolerance and restraining tissue inflammation, and that Tim-1 signaling-dependent TIGIT expression on B cells is essential for maintaining CNS-specific tolerance. A possible critical role of aryl hydrocarbon receptor (AhR) in regulating the B cell function is discussed, as we find that AhR is among the preferentially expressed transcription factors in Tim-1$^+$ B cells and regulates their TIGIT and IL-10 expression.

INTRODUCTION

Tim-1 is expressed in immune cells and regulates their responses in a cell intrinsic manner (Kuchroo et al., 2008; Rennert, 2011). Tim-1$^+$ B cells can suppress effector T cell responses in experimental models of autoimmunity, allograft rejection, and allergic airway inflammation (Ding et al., 2011; Xiao et al., 2012, 2015; Yeung et al., 2015). As a phosphatidylserine receptor, Tim-1 expression on B cells is required for optimal interleukin 10 (IL-10) production by binding to apoptotic cells (ACs; Xiao et al., 2015), and IL-10$^+$ B cells are enriched within Tim-1$^+$ cells in both mice and humans (Ding et al., 2011; Gu et al., 2017; Liu et al., 2014; Xiao et al., 2012, 2015). Dysregulated IL-10$^+$Tim-1$^+$ B cell populations have been associated with inflammatory diseases in humans (Ma et al., 2014; Aravena et al., 2017; Gu et al., 2017; Kristensen et al., 2015; Liu et al., 2014; Mao et al., 2017). Although IL-10 has been suggested as a primary effector for the regulatory function of B cells, nevertheless mice with B cell-specific IL-10 deletion do not develop spontaneous inflammation with age (Madan et al., 2009). We previously reported that Tim-1 mutant mice developed sporadic spontaneous inflammation in multiple organs; however, from these studies it was not clear whether the effect was solely due to loss of Tim-1 function on B cells and what was the molecular mechanism by which Tim-1$^+$ B cells mediated their regulatory function. Here we have provided evidence supporting that Tim-1$^+$ B cells, whose function requires Tim-1 expression and signaling, are critical for maintaining self-tolerance and limiting tissue inflammation and that this non-redundant regulatory function for Tim-1$^+$ B cells is partly mediated by expressing the checkpoint receptor TIGIT.

RESULTS

Tim-1^{BKO} Mice Develop Spontaneous Multi-organ Tissue Inflammation with Age

To firmly evaluate the role of Tim-1 in B cells, we generated Tim-1 floxed (Tim-1$^{fl/fl}$) mice (Figure 1A) and crossed them with CD19$^{Cre/Cre}$ mice (Rickert et al., 1997) to produce

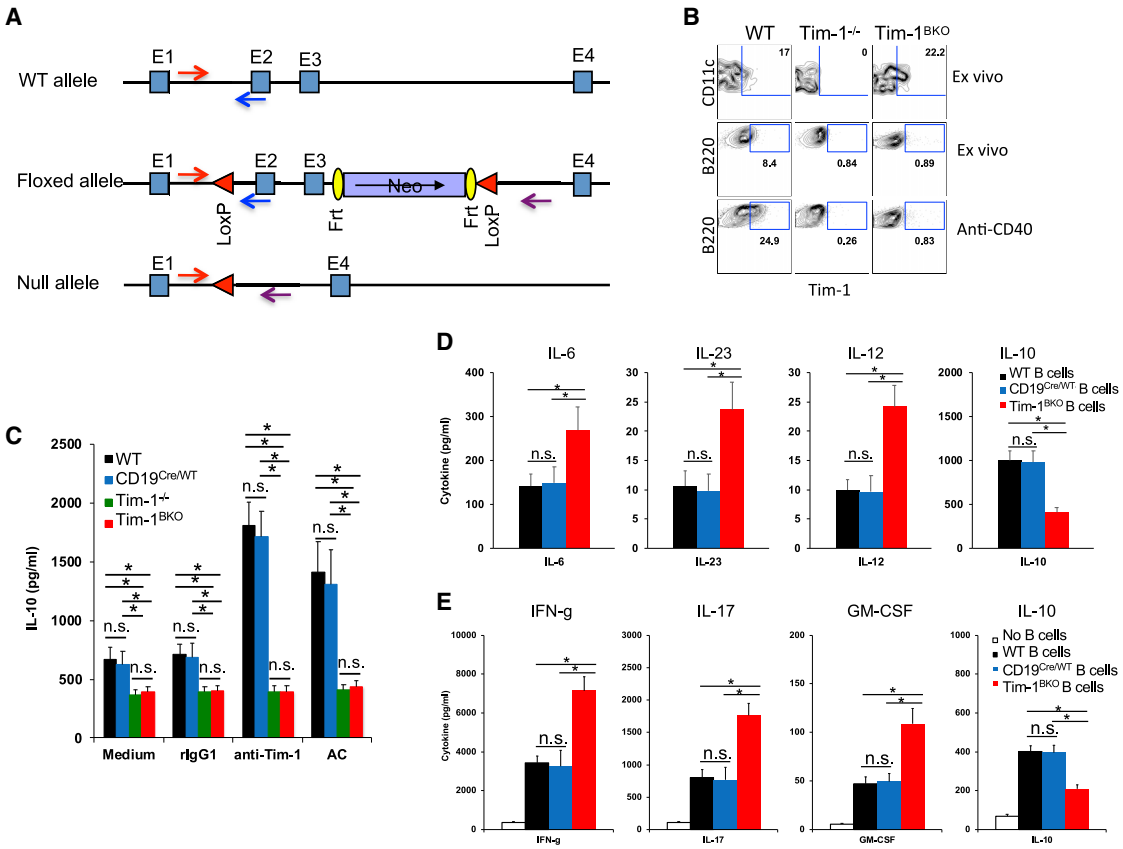

Figure 1. Generation of Tim-1^{BKO} Mice

(A) Strategy for generating Tim-1 floxed mice.

(B) Representative fluorescence-activated cell sorting (FACS) plots showing Tim-1 expression in dendritic cells (DCs) and B cells in spleens of 6- to 8-week-old mice (n = 6–8) *ex vivo* or in isolated B cells activated with anti-CD40 for two days.

(C) B cells isolated from 6- to 8-week-old mice (n = 5–6 per group) were cultured with anti-Tim-1, apoptotic cells (ACs), or controls. After 60 h, IL-10 production in culture supernatants was measured by ELISA.

(D) B cells isolated from 6- to 8-week-old mice (n = 5–8 per group) were cultured with lipopolysaccharide (LPS) for 40 h and then examined for their cytokine production in culture supernatants by BioLegend LEGENDplex.

(E) Foxp3^{-} T cells from 6- to 8-week-old Foxp3-GFP knockin (KI) mice were cultured with B cells from WT or Tim-1^{BKO} mice (n = 5 per group) plus soluble anti-CD3 for three days. Then, isolated T cells from the cultures were re-activated with plate-bound anti-CD3, and cytokine production in 40-h cultures was measured by BioLegend LEGENDplex. *p < 0.01; n.s., not significant. Data are represented as mean ± SEM.

See also Figure S1.

CD19$^{Cre/WT}$Tim-1$^{fl/fl}$ (Tim-1^{BKO}) mice. We confirmed that Tim-1 was effectively deleted only in B cells in Tim-1^{BKO} mice (Figure 1B); Tim-1^{BKO} B cells stimulated with anti-Tim-1 or ACs had both reduced basal and induced IL-10 production (Figure 1C); LPS-activated Tim-1^{BKO} B cells produced less IL-10, but more proinflammatory cytokines IL-6, IL-23, and IL-12 (Figure 1D). Consequently, Tim-1^{BKO} B cells as antigen-presenting cells (APCs) promoted T cell production of the inflammatory cytokines interferon γ (IFN-γ), IL-17, and granulocyte-macrophage colony-stimulating factor (GM-CSF), but inhibited IL-10 production (Figure 1E). The data support that Tim-1 expression on B cells determines inflammatory cytokine responses.

Tim-1^{BKO} mice at <6 months of age appeared normal clinically and histologically, and did not display gross differences in T/B cells, macrophages, or dendritic cells (Figure S1). Interestingly, with age Tim-1^{BKO} mice developed multi-organ tissue inflammation. About 65% of 10^{+}-months-old Tim-1^{BKO} mice showed clinical abnormalities, including weight loss and/or rectal prolapse (27%), dermatitis (19%), and strikingly, spontaneous experimental autoimmune encephalomyelitis (EAE)-like paralytic disease (19%; Figure 2A). Histological examination of livers, lungs, kidneys, intestines, and central nervous system (CNS) showed that 100% of aged Tim-1^{BKO} mice had immune cell infiltrates in one or more of these organs: liver (88.5%), lungs (88.5%), kidney (96.2%), intestines (92.3%), and CNS (26.9%; Figures 2A, 2B, and S2). Some Tim-1^{BKO} mice with paralysis displayed meningeal granulomatous inflammation in the CNS with Touton giant cells, whose appearance is indicative of hyperactivation of proinflammatory myeloid cells (Figure 2B).These data suggest that with age, loss of Tim-1 expression in B cells leads to a broad defect in maintenance of tolerance in multiple organs and tissues, even including the CNS.

CellPress
OPEN ACCESS

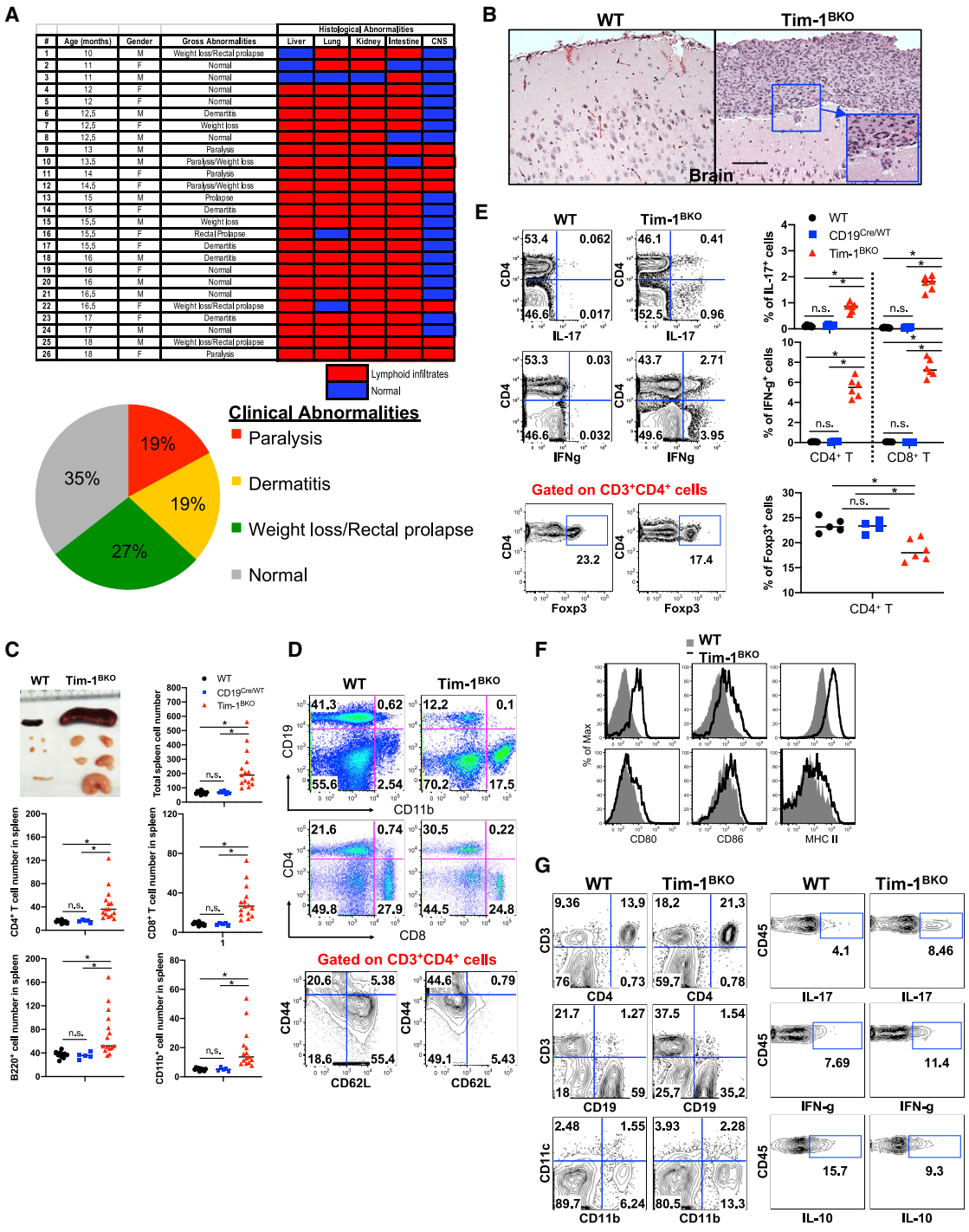

Figure 2. Aged Tim-1^{BKO} Mice Develop Spontaneous Tissue Inflammation

(A) Table and graphs summarize clinical and histological abnormalities in 10- to 18-month-old Tim-1^{BKO} mice.

(B) A Tim-1^{BKO} mouse (#12 in A showed granulomatous inflammation in brain leptomeninges. Boxed area indicates a Touton giant cell shown at higher magnification. Bar, 100 μm.

(C) Tim-1^{BKO} mice showed enlarged spleens and lymph nodes (LNs). Total splenocyte numbers were determined by trypan blue exclusion.

(D) Representative FACS plots showing phenotypes of immune cells (upper and middle panels) and CD4$^+$ T cell activation (lower panels, gated CD3$^+$CD4$^+$ cells).

(E) Representative FACS plots showing phenotypes of T cell cytokine production (upper and middle panels, gated CD3$^+$ cells) and Foxp3$^+$ Tregs (lower panels, gated CD3$^+$CD4$^+$ cells).

(legend continued on next page)

Aged Tim-1^{BKO} mice also had lymphadenopathy and splenomegaly with a 2- to 8-fold increase in immune cells, predominantly CD11b$^+$ cells, CD4$^+$ and CD8$^+$ T cells, and B220$^+$ B cells, compared to control (wild-type [WT], CD19$^{Cre/WT}$, and CD19$^{Cre/WT}$Tim-1$^{fl/WT}$) mice (Figures 2C and 2D). T cells from the Tim-1^{BKO} mice displayed a more activated/memory-like phenotype (CD44^{hi}CD62L^{low}; Figure 2D) with increased IFN-γ and IL-17 production, but decreased frequency of Foxp3$^+$ Tregs (Figure 2E). Aged Tim-1^{BKO} mice also displayed increased activation of CD11c$^+$ dendritic cells and especially B cells, with increased expression of major histocompatibility complex (MHC) II and costimulatory molecules CD80 and CD86 (Figure 2F). Tim-1^{BKO} mice with rectal prolapse showed predominantly increased T cells and CD11b$^+$ myeloid cells in colonic lamina propria, and their CD4$^+$ T cells produced more IFN-γ and IL-17 but less IL-10 (Figure 2G). Thus, B cell expression of Tim-1 is required for maintenance of tolerance, and loss of Tim-1 expression in the B cells results in the development of multi-organ inflammation accompanied by increased activation of and production of proinflammatory cytokines by T cells, B cells, and myeloid cells.

Tim-1^{BKO} Mice Develop More Severe MOG$_{35–55}$-Induced EAE

As aged Tim-1^{BKO} mice developed spontaneous paralysis with inflammation in the CNS, we asked whether B cell deficiency of Tim-1 would affect EAE induction in young mice that did not yet display inflammation. Indeed, following immunization with MOG$_{35–55}$, young Tim-1^{BKO} mice developed more severe clinical signs of EAE with poorer recovery (Figures 3A and S3A), associated with increased frequencies of IFN-γ^+ and IL-17$^+$ T cells, and reduced frequencies of Foxp3$^+$ Tregs and IL-10$^+$ T cells in the CNS (Figure 3B), supporting our previous observation that B cell Tim-1 expression is essential for regulating the balance of proinflammatory Th1/Th17 cells and regulatory Foxp3$^+$ Tregs and IL-10$^+$ Tr1 cells (Xiao et al., 2015), and thus the development of autoimmunity.

Tim-1$^+$ B Cells Highly Express a Set of Negative Immune Regulators besides IL-10

To gain more insights into the mechanism by which Tim-1$^+$ B cells mediate their inhibitory function, we performed RNA sequencing (RNA-seq) analysis on highly purified Tim-1$^+$ and Tim-1$^-$ B cells from naive WT mice. Of the 15,519 genes detected, 888 were significantly differentially expressed between Tim-1$^+$ and Tim-1$^-$ B cells—768 genes were upregulated in Tim-1$^+$ B cells, while 120 were downregulated (Figure 3C). Interestingly, besides expressing *Tim-1* and *IL10*, Tim-1$^+$ B cells also express many of the molecules that have previously been identified as markers for various IL-10$^+$ Breg cell populations (e.g., CD9, CD25, CD44/CD138, and CD5/CD1d; Mauri and Menon, 2015; Sun et al., 2015) or as important for the function of IL-10$^+$ B cells (e.g., CD80 and CD86; Mann et al., 2007; Figure 3D). In addition to *IL10*, Tim-1$^+$ B cells also highly expressed a panel of other negative immune modulators including *Ebi3* (a subunit of IL-27), *Entpd1* (encoding CD39), *Nt5e* (encoding CD73), *Gitrl*, and *Fgl2*. Interestingly, Tim-1$^+$ B cells also highly expressed a set of checkpoint receptors including *Tigit*, *CTLA4*, *Lag3*, *Pdcd1* (encoding PD-1), and *Havcr2* (encoding *Tim-3*; Figures 3E and S3B) that have been associated with CD8$^+$ T cell exhaustion/dysfunction and with Treg function, and therefore with self-tolerance and regulation of inflammation and autoimmunity (Anderson et al., 2016; Joller et al., 2012; Kuchroo et al., 2014).

Tim-1$^{\Delta mucin}$ is a loss-of-function Tim-1 mutant still expressed on the cell surface and can be stained with anti-Tim-1 (Xiao et al., 2012, 2015), thus providing a valuable tool for identifying Tim-1$^{\Delta mucin+}$ cells and for studying the effect of loss of Tim-1 signaling on B cell function. Using B cells from Tim-1$^{\Delta mucin}$ mice, we found that loss of Tim-1 signaling (Tim-1$^{\Delta mucin}$) did not alter expression of those genes previously identified as markers for various IL-10$^+$ B cell subsets (e.g., CD9, CD5/CD1d, and CD138/CD44) or some genes previously reported to be involved in B cell regulatory function (e.g., *Entpd1*, *Nt5e*, *Gitrl*, and *Ebi3*). Interestingly however, in addition to *IL10*, expression of the checkpoint receptors *Tigit*, *Tim-3*, *Lag3*, and *Ctla4*, but not *Pdcd1*, was significantly reduced in Tim-1$^{\Delta mucin+}$ cells, of which *Tigit* expression was most dramatically reduced (Figure 3F), indicating that their expression requires Tim-1 signaling. As Tim-1$^+$ B cells highly express IL-10 as well as a panel of negative immune regulators, this suggests that Tim-1$^+$ B cells may maintain self-tolerance and suppress inflammation by using multiple regulatory mechanisms, e.g., by expressing checkpoint receptors.

Role of TIGIT in B Cell Function

TIGIT is expressed on natural killer (NK) and T cells and is important for regulating immune responses in autoimmunity and cancer (Anderson et al., 2016; Joller et al., 2012; 2014). Here we found that TIGIT was also expressed in B cells and enriched in Tim-1$^+$ B cells (Figures 3E and 3F). Tim-1 ligation with an anti-Tim-1 monoclonal antibody (mAb) increased TIGIT expression and IL-10 production from B cells (Figure 4A), supporting the idea that Tim-1 signaling in B cells positively regulates TIGIT and IL-10 expression. Interestingly, we found that AhR is preferentially expressed in Tim-1$^+$ B cells and required for their regulatory function. and for Tim-1-mediated expression of TIGIT and IL-10 by directly binding to their promoters in the B cells (Figure S4). Although TIGIT and IL-10 are mostly co-expressed, about 25% to 30% of TIGIT$^+$ B cells are IL-10$^-$ and many of the IL-10$^+$ cells are TIGIT$^-$, indicating that expression of TIGIT and IL-10 can be separable events. Interestingly, while IL-10 blockade with anti-IL-10 mAb did not affect basal or Tim-1 ligation-induced TIGIT expression in B cells (Figure S5A), B cells from TIGIT-deficient (Tigit$^{-/-}$) mice produced less IL-10 upon treatment with a number of stimuli, indicating that B cells may

(F) Representative FACS plots showing phenotypes of B cells (upper panel, gated CD19$^+$ cells) and DCs (lower panel, gated CD11c$^+$ cells) in LNs from control and Tim-1^{BKO} mice (n = 5–15).

(G) Representative FACS data showing immune cell phenotypes in colonic LP of Tim-1^{BKO} mice (n = 4). (Left panels) Gated CD45$^+$ cells. (Right panels) Gated CD45$^+$CD3$^+$CD4$^+$cells. *p < 0.01; n.s., not significant. Data are represented as mean ± SEM.

See also Figure S2.

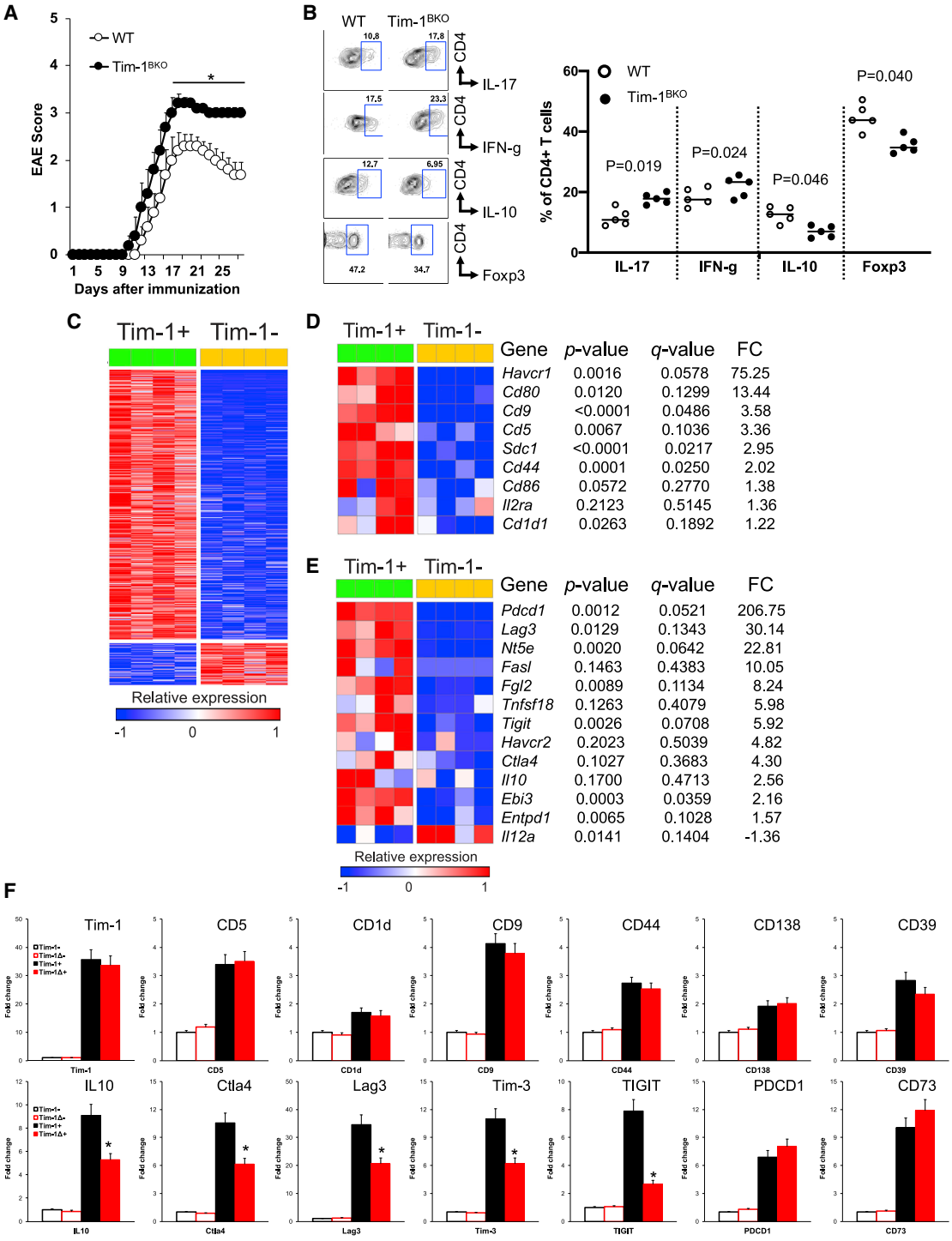

Figure 3. Young Tim-1^{BKO} Mice Develop More Severe EAE, and Tim-1^{+} B Cells Differentially Express a Set of Co-inhibitory Molecules besides IL10

(A) 6- to 8-week-old mice were immunized with $MOG_{35–55}$/CFA (Complete Freund's Adjuvant) and scored daily for clinical EAE signs (n = 10/group). *$p < 0.05$.

(B) Thirty days after EAE induction, Foxp3 and cytokine expression in CNS-infiltrating CD4^{+} T cells was determined by flow cytometry.

(C) Heatmap showing differentially expressed genes from RNA-seq analysis of splenic Tim-1^{-} and Tim-1^{+} B cells from 8-week-old naive WT mice (asymptotic Student's t test $p \leq 0.05$, absolute fold change ≥ 2).

(D) Heatmap of selected genes from (C) showing expression of known cell surface molecules associated with IL-10^{+} B cell subsets in Tim-1^{+} versus Tim-1^{-} B cells.

(legend continued on next page)

require TIGIT for optimal IL-10 production (Figure 4B). We then examined whether Tim-1$^+$ B cells from Tigit$^{-/-}$ mice affect EAE development. As we reported previously, transfer of WT Tim-1$^+$ B cells significantly inhibited EAE severity (Xiao et al., 2015). Transfer of Tigit$^{-/-}$ Tim-1$^+$ B cells also suppressed disease severity, but not as effectively as transfer of WT Tim-1$^+$ B cells (Figure S5B), indicating that TIGIT is required for some of the regulatory activities of Tim-1$^+$ B cells in suppressing inflammation. To further understand the role of TIGIT in B cells *in vivo*, we generated Tigit$^{fl/fl}$ mice (Figure S5C) and crossed them with CD19$^{Cre/Cre}$ mice to obtain mice lacking TIGIT specifically in B cells (CD19$^{Cre/WT}$Tigit$^{fl/fl}$ or Tigit^{BKO}). Efficient TIGIT deletion in B cells was confirmed by flow cytometry (Figure S5D). Up to 5 to 6 months of age, Tigit^{BKO} mice displayed a normal phenotype without any notable defects in Tim-1 expression in B cells or B cell development (Figures S5E and S5F). When immunized with $MOG_{35–55}$, WT, CD19$^{Cre/WT}$, and CD19$^{Cre/WT}$Tigit$^{fl/WT}$ showed comparable EAE development and severity. Compared to these control mice, young Tigit^{BKO} mice developed more severe EAE, with poorer recovery (Figure 4C), similar to Tim-1^{BKO} mice (Figure 3A), indicating an important role of TIGIT in B cells in inhibiting CNS inflammation. Unlike Tim-1^{BKO} mice, Tigit^{BKO} mice with age did not show clinical signs of dermatitis, weight loss, or rectal prolapse (Figure 4D). Interestingly, however, similar to Tim-1^{BKO} mice, about 20% of Tigit^{BKO} mice developed spontaneous EAE-like paralytic disease (Figure 4D and Video S1). Histological examination of liver, lungs, kidneys, intestines, and CNS in aged Tigit^{BKO} mice revealed that 50% of the mice had lymphoid infiltrates in various organs/tissues, in contrast to 100% observed in Tim-1^{BKO} mice (Figure 4D). Aged Tigit^{BKO} mice also had fewer and smaller foci of mononuclear cell infiltrates in livers, lungs, kidneys, and colons than Tim-1^{BKO} mice (Figure 4E).

Additionally, the incidence of histopathological tissue inflammation in liver (33.3% versus 88.5%), lungs (33.3% versus 88.5%), intestines (44.4% versus 92.3%), and kidneys (5.6% versus 96.2%) of aged Tigit^{BKO} mice was much lower than that in aged Tim-1^{BKO} mice (Figures 4D, 2A, and S5G), and inflammation was less widespread, as aged Tigit^{BKO} mice only had lymphoid infiltrates in two (22.2%) or three (22.2%) organs/tissues (Figure 4D), whereas 80.7% of aged Tim-1^{BKO} mice had lymphoid infiltrates in four or five organs/tissues (Figure 2A). As aged Tigit^{BKO} and Tim-1^{BKO} mice had a comparable incidence of spontaneous paralysis, we examined the brain infiltrates in the mice with paralysis and found that both strains with paralysis showed about a 4-fold increase of immune cell infiltrates brains, with increased T cells and especially CD11b$^+$ myeloid cells, and a decreased frequency of Foxp3$^+$ Tregs (Figure 4F). Young Tigit^{BKO} mice, like young Tim-1^{BKO} mice, showed no defect in Treg frequency, surface CTLA-4, CD39, and CD73 expression, or suppressive capacity, compared to control (Figures S5H–S5J).

Examination of peripheral immune compartments in aged Tigit^{BKO} mice demonstrated that those mice without organ/tissue inflammation had no obvious changes in immune cell infiltrates, compared to control mice. In contrast, T cells from spleens of aged Tigit^{BKO} mice with CNS infiltrates and paralysis were more activated and produced more IFN-γ and IL-17. Also, levels of CD11b$^+$ myeloid cells were increased, but there was no change in the frequency of Foxp3$^+$ Tregs (Figure S5K).

Collectively, these data support that TIGIT, a checkpoint receptor differentially expressed on Tim-1$^+$ B cells and induced by Tim-1 signaling, is not only critical for B cell-mediated suppression of inflammation, it is also required for B cell-mediated induction of tolerance, especially in the CNS.

DISCUSSION

Tim-1 is broadly expressed on multiple cell types and regulates multiple biological functions (Bonventre, 2014; Kuchroo et al., 2008; Rennert, 2011; Xiao et al., 2011). Here we have shown that over 80% of Tim-1^{BKO} mice developed spontaneous multi-organ tissue inflammation as they age, clearly demonstrating that Tim-1 expression on B cells is required for maintaining self-tolerance. Surprisingly, 27% of the Tim-1^{BKO} mice developed a spontaneous paralysis, indicating that the selective loss of Tim-1 on B cells is unique in protecting mice from the development of CNS inflammation, even without immunization with a CNS antigen or expression of a CNS antigen-specific TCR or BCR. This emphasizes that in addition to their critical regulatory role in maintaining self-tolerance systemically, Tim-1$^+$ B cells have a unique role in maintaining tolerance in the CNS.

Although also targeting CD20 expressing CD8$^+$ T cells (Sabatino et al., 2019), the efficacy of anti-CD20 therapy in multiple sclerosis has been mainly attributed to deletion of proinflammatory B cells and induction of "regulatory" B cells, as the immune system resets itself to replenish B cells in the repertoire (Li et al., 2016). Tim-1 is expressed in ~10% of B cells, yet Tim-1^{BKO} mice developed both spontaneous and more severe induced CNS inflammation, supporting that Tim-1$^+$ B cells may be critical in this context and that Tim-1 signaling is essential for regulating the balance between "regulatory" and proinflammatory B cells in order to maintain self-tolerance in tissues including the CNS.

Besides IL-10, Tim-1$^+$ B cells also differentially express a panel of negative immune regulators, including a set of checkpoint receptors that likely contribute to the regulatory function of Tim-1$^+$ B cells. In support of this, TIGIT^{BKO} mice, with age, preferentially develop spontaneous paralytic disease with CNS inflammation. It should be emphasized that development of spontaneous paralytic disease with CNS inflammation has not been observed previously in mice with global loss of negative regulatory molecules, including IL-10, CTLA-4, TIGIT, PD-1, or Tim-3. The checkpoint receptors not only induce CD8$^+$ T cell exhaustion, but also enhance the regulatory function of Foxp3$^+$ Tregs. As we have observed a similar set of checkpoint receptors expressed on Tim-1$^+$ B cells that regulate tissue inflammation, this raises an interesting question of whether checkpoint

(E) Heatmap of selected genes from (C) showing expression of well-known negative immune regulators in Tim-1$^+$ versus Tim-1$^-$ B cells.
(F) qPCR data of selected genes in WT Tim-1$^-$ and Tim-1$^+$ B cells and Tim-1$^{\Delta mucin-}$ and Tim-1$^{\Delta mucin+}$ B cells, normalized to expression in WT Tim-1$^-$ B cells. *$p < 0.01$ (Tim-1$^+$ versus Tim-1$^{\Delta mucin+}$ cells; n = 4). Data are represented as mean ± SEM.
See also Figure S3.

CellPress
OPEN ACCESS

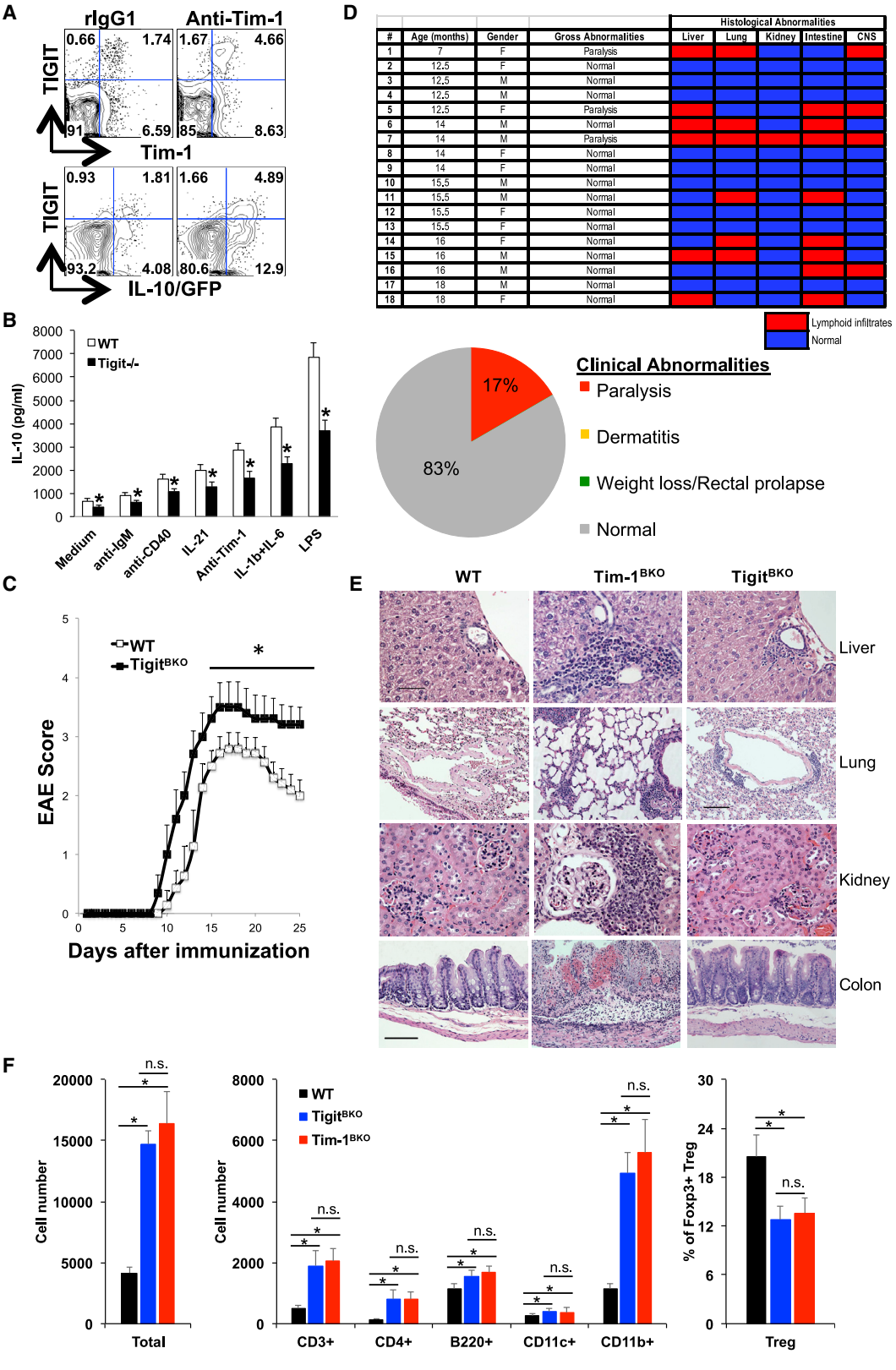

(legend on next page)

blockade-induced anti-tumor immunity may also alter the regulatory function of B cells that express these checkpoint receptors.

Our data suggest that Tim-1$^+$ B cells must limit inflammation through diverse regulatory mechanisms, and we speculate that individual regulatory mechanisms may be operational in a particular tissue and inflammatory setting. TIGIT appears to be preferentially required for Tim-1$^+$ B cell-mediated self-tolerance in the CNS, and by analogy, there must be other regulatory mechanisms (preferentially or coordinately) responsible for Tim-1$^+$ B cell-mediated self-tolerance in other organs and tissues. Alternatively, loss of individual effector mechanism in Tim-1$^+$ B cells may only have a limited effect on the regulation of tissue inflammation, but multiple mechanisms may be coordinately working together in the B cells to regulate tissue inflammation in multiple organs or multiple tissue specificities.

A recent study has identified AhR as a critical transcription factor (TF) for the regulatory function of IL-10$^+$ B cells by directly regulating IL-10 and suppressing proinflammatory gene expression (Piper et al., 2019). We also found that AhR is preferentially expressed and ranks at the top among TFs expressed in Tim-1$^+$ B cells (Figure S4A). Maintenance and induction of AhR in these B cells require Tim-1 expression and signaling (Figure S4B). AhR is required for Tim-1-mediated expression of IL-10 and TIGIT by directly binding to their promoters in the B cells (Figures S4C–S4E). Importantly, AhR is required for the regulatory function of Tim-1$^+$ B cells in ameliorating EAE severity (Figure S4F). It is possible that AhR in Tim-1$^+$ B cells also regulates other regulatory mechanisms, besides IL-10 and TIGIT. In this regard, our computational analysis has identified putative AhR-binding sites in the promoter regions of other coinhibitory molecules such as Tim-3 and LAG3. Thus, it is very likely that AhR may serve as a critical TF responsible for the regulatory activity of Tim-1$^+$ B cells by directly regulating the module of negative regulators and suppressing proinflammatory factors by binding to their promoters in these cells. In addition to AhR, our RNA-seq analysis has also identified a set of other TFs preferentially expressed in Tim-1$^+$ B cells; however, whether any of these TFs is also required for Tim-1$^+$ B cell regulatory function, needs further investigation.

In summary, we demonstrate that Tim-1$^+$ B cells are essential in maintaining self-tolerance and restraining tissue inflammation, and that the Tim-1/TIGIT axis is required for their optimal regulatory function, especially for maintaining tolerance in the CNS. The regulatory function of Tim-1$^+$ B cells has also been identified in infections and transplantation (Ding et al., 2011; Liu et al., 2014; Mao et al., 2017). Thus, further understanding Tim-1$^+$ B cells and their regulatory mechanisms would be valuable for treating immune-related diseases by selectively enhancing or inhibiting the B cell activity and/or their regulatory mechanisms.

STAR★METHODS

Detailed methods are provided in the online version of this paper and include the following:

- KEY RESOURCES TABLE
- RESOURCE AVAILABILITY
  - Lead Contact
  - Materials Availability
  - Data and Code Availability
- EXPERIMENTAL MODEL AND SUBJECT DETAILS
  - Animals
- METHOD DETAILS
  - Cell purification and cultures
  - Flow cytometry
  - EAE
  - Chromatin immunoprecipitation (ChIP)
  - RNA isolation, real-time PCR, and histology
  - RNA-seq assay
- QUANTIFICATION AND STATISTICAL ANALYSIS

SUPPLEMENTAL INFORMATION

Supplemental Information can be found online at https://doi.org/10.1016/j.celrep.2020.107892.

ACKNOWLEDGMENTS

We thank Deneen Kozoriz for cell sorting and Dr. Mary Collins for advice and editing the paper. This work was supported by grants from the Lupus Research Alliance (332938 to S.X.), the National MS Society (RG-1907-34686), and the National Institutes of Health (P01AI039671, P01AI045757, P01073748, and 1P01AI129880 to V.K.K.). N.J. is supported by the Swiss National Science Foundation (PP00P3_150663) and the European Research Council (677200). V.K.K is the Dr. William E. Paul Distinguished Innovator Award recipient from the Lupus Research Alliance.

AUTHOR CONTRIBUTIONS

S.X. designed and performed experiments and wrote the paper; N.P., D.H., and A.M. analyzed RNA-seq data; L.B., S.B.K., J.K., A.H., R.S., T.-B.-S.,

Figure 4. Immunoregulatory Role of TIGIT in B Cells

(A) Representative FACS plots showing Tim-1, TIGIT, and IL-10-GFP expression in splenic CD19$^+$ B cells from 8-week-old IL10^{GFP} tiger mice (n = 6) after cells were treated with anti-Tim-1 or control rIgG1 for three days.

(B) Splenic B cells from 8-week-old WT and Tigit$^{-/-}$ mice were treated with indicated stimuli for three days and IL-10 production in culture supernatants was measured by ELISA. *p < 0.01.

(C) 8-week-old mice were immunized with MOG$_{35-55}$/CFA and scored daily for clinical EAE signs (n = 10 per group; *p < 0.05).

(D) Table and graph summarizing clinical and histological abnormalities in Tigit^{BKO} mice.

(E) Representative histological examination of indicated organs/tissues in Tigit^{BKO} and Tim-1^{BKO} mice. Tim-1^{BKO} mice showed marked lymphoid infiltrates in periportal areas of the liver, peribronchial areas, renal cortex, lamina propria, and submucosal areas of the large intestine. The extent of infiltration was much less in tissues of Tigit^{BKO} mice. No tissue inflammation was present in WT mice. Bar in the liver panel, 50 μm, applies to liver and kidney tissue panels; bar in the lung panels, 100 μm, applies to the lung tissue panels; bar in the intestine panel, 100 μm, applies to the intestine tissue panels.

(F) Phenotypes of brain-infiltrating immune cells determined by flow cytometry in WT (n = 9), Tigit^{BKO} (n = 4), and Tim-1^{BKO} (n = 5) mice with spontaneous EAE-like paralysis. *p < 0.01; n.s., not significant. Data are represented as mean ± SEM.

See also Figures S4 and S5.

J.S., H.Z., F.J.Q., and N.J. performed experiments; V.K.K. supervised the study and edited the paper.

DECLARATION OF INTERESTS

S.X. is the employee of Celsius Therapeutics. V.K.K. has an ownership interest and is a member of the SAB for Celsius Therapeutics and Tizona Therapeutics. V.K.K.'s interests were reviewed and managed by the Brigham and Women's Hospital and Partners Healthcare in accordance with their conflict of interest policies. A provisional patent application was filed including work of this paper.

Received: April 16, 2019
Revised: December 6, 2019
Accepted: June 19, 2020
Published: July 14, 2020

REFERENCES

Anderson, A.C., Joller, N., and Kuchroo, V.K. (2016). Lag-3, Tim-3, and TIGIT: co-inhibitory receptors with specialized functions in immune regulation. Immunity *44*, 989–1004.

Aravena, O., Ferrier, A., Menon, M., Mauri, C., Aguillón, J.C., Soto, L., and Catalán, D. (2017). TIM-1 defines a human regulatory B cell population that is altered in frequency and function in systemic sclerosis patients. Arthritis Res. Ther. *19*, 8.

Bonventre, J.V. (2014). Kidney injury molecule-1: a translational journey. Trans. Am. Clin. Climatol. Assoc. *125*, 293–299.

Ding, Q., Yeung, M., Camirand, G., Zeng, Q., Akiba, H., Yagita, H., Chalasani, G., Sayegh, M.H., Najafian, N., and Rothstein, D.M. (2011). Regulatory B cells are identified by expression of TIM-1 and can be induced through TIM-1 ligation to promote tolerance in mice. J. Clin. Invest. *121*, 3645–3656.

Gu, X.L., He, H., Lin, L., Luo, G.X., Wen, Y.F., Xiang, D.C., and Qiu, J. (2017). Tim-1^{+} B cells suppress T cell interferon-gamma production and promote Foxp3 expression, but have impaired regulatory function in coronary artery disease. APMIS *125*, 872–879.

Joller, N., Peters, A., Anderson, A.C., and Kuchroo, V.K. (2012). Immune checkpoints in central nervous system autoimmunity. Immunol. Rev. *248*, 122–139.

Joller, N., Lozano, E., Burkett, P.R., Patel, B., Xiao, S., Zhu, C., Xia, J., Tan, T.G., Sefik, E., Yajnik, V., et al. (2014). Treg cells expressing the coinhibitory molecule TIGIT selectively inhibit proinflammatory Th1 and Th17 cell responses. Immunity *40*, 569–581.

Kim, D., Pertea, G., Trapnell, C., Pimentel, H., Kelley, R., and Salzberg, S.L. (2013). TopHat2: accurate alignment of transcriptomes in the presence of insertions, deletions and gene fusions. Genome Biol. *14*, R36.

Kristensen, B., Hegedüs, L., Lundy, S.K., Brimnes, M.K., Smith, T.J., and Nielsen, C.H. (2015). Characterization of regulatory B cells in Graves' disease and Hashimoto's thyroiditis. PLoS ONE *10*, e0127949.

Kuchroo, V.K., Dardalhon, V., Xiao, S., and Anderson, A.C. (2008). New roles for TIM family members in immune regulation. Nat. Rev. Immunol. *8*, 577–580.

Kuchroo, V.K., Anderson, A.C., and Petrovas, C. (2014). Coinhibitory receptors and CD8 T cell exhaustion in chronic infections. Curr. Opin. HIV AIDS *9*, 439–445.

Li, R., Rezk, A., Healy, L.M., Muirhead, G., Prat, A., Gommerman, J.L., and Bar-Or, A.; MSSRF Canadian B Cells in MS Team (2016). Cytokine-defined B cell responses as therapeutic targets in multiple sclerosis. Front. Immunol. *6*, 626.

Liu, J., Zhan, W., Kim, C.J., Clayton, K., Zhao, H., Lee, E., Cao, J.C., Ziegler, B., Gregor, A., Yue, F.Y., et al. (2014). IL-10-producing B cells are induced early in HIV-1 infection and suppress HIV-1-specific T cell responses. PLoS ONE *9*, e89236.

Ma, L., Liu, B., Jiang, Z., and Jiang, Y. (2014). Reduced numbers of regulatory B cells are negatively correlated with disease activity in patients with new-onset rheumatoid arthritis. Clin. Rheumatol. *33*, 187–195.

Madan, R., Demircik, F., Surianarayanan, S., Allen, J.L., Divanovic, S., Trompette, A., Yogev, N., Gu, Y., Khodoun, M., Hildeman, D., et al. (2009). Nonredundant roles for B cell-derived IL-10 in immune counter-regulation. J. Immunol. *183*, 2312–2320.

Mann, M.K., Maresz, K., Shriver, L.P., Tan, Y., and Dittel, B.N. (2007). B cell regulation of CD4+CD25+ T regulatory cells and IL-10 via B7 is essential for recovery from experimental autoimmune encephalomyelitis. J. Immunol. *178*, 3447–3456.

Mao, H., Pan, F., Wu, Z., Wang, Z., Zhou, Y., Zhang, P., Gou, M., and Dai, G. (2017). Colorectal tumors are enriched with regulatory plasmablasts with capacity in suppressing T cell inflammation. Int. Immunopharmacol. *49*, 95–101.

Mauri, C., and Menon, M. (2015). The expanding family of regulatory B cells. Int. Immunol. *27*, 479–486.

Picelli, S., Björklund, A.K., Faridani, O.R., Sagasser, S., Winberg, G., and Sandberg, R. (2013). Smart-seq2 for sensitive full-length transcriptome profiling in single cells. Nat. Methods *10*, 1096–1098.

Piper, C.J.M., Rosser, E.C., Oleinika, K., Nistala, K., Krausgruber, T., Rendeiro, A.F., Banos, A., Drozdov, I., Villa, M., Thomson, S., et al. (2019). Aryl hydrocarbon receptor contributes to the transcriptional program of IL-10-producing regulatory B cells. Cell Rep. *29*, 1878–1892 e7.

Reich, M., Liefeld, T., Gould, J., Lerner, J., Tamayo, P., and Mesirov, J.P. (2006). GenePattern 2.0. Nat. Genet. *38*, 500–501.

Rennert, P.D. (2011). Novel roles for TIM-1 in immunity and infection. Immunol. Lett. *141*, 28–35.

Rickert, R.C., Roes, J., and Rajewsky, K. (1997). B lymphocyte-specific, Cre-mediated mutagenesis in mice. Nucleic Acids Res. *25*, 1317–1318.

Sabatino, J.J., Jr., Wilson, M.R., Calabresi, P.A., Hauser, S.L., Schneck, J.P., and Zamvil, S.S. (2019). Anti-CD20 therapy depletes activated myelin-specific CD8^{+} T cells in multiple sclerosis. Proc. Natl. Acad. Sci. USA *116*, 25800–25807.

Sun, J., Wang, J., Pefanis, E., Chao, J., Rothschild, G., Tachibana, I., Chen, J.K., Ivanov, I.I., Rabadan, R., Takeda, Y., and Basu, U. (2015). Transcriptomics identify CD9 as a marker of murine IL-10-competent regulatory B cells. Cell Rep. *13*, 1110–1117.

Trapnell, C., Roberts, A., Goff, L., Pertea, G., Kim, D., Kelley, D.R., Pimentel, H., Salzberg, S.L., Rinn, J.L., and Pachter, L. (2012). Differential gene and transcript expression analysis of RNA-seq experiments with TopHat and Cufflinks. Nat. Protoc. *7*, 562–578.

Xiao, S., Zhu, B., Jin, H., Zhu, C., Umetsu, D.T., DeKruyff, R.H., and Kuchroo, V.K. (2011). Tim-1 stimulation of dendritic cells regulates the balance between effector and regulatory T cells. Eur. J. Immunol. *41*, 1539–1549.

Xiao, S., Brooks, C.R., Zhu, C., Wu, C., Sweere, J.M., Petecka, S., Yeste, A., Quintana, F.J., Ichimura, T., Sobel, R.A., et al. (2012). Defect in regulatory B-cell function and development of systemic autoimmunity in T-cell Ig mucin 1 (Tim-1) mucin domain-mutant mice. Proc. Natl. Acad. Sci. USA *109*, 12105–12110.

Xiao, S., Brooks, C.R., Sobel, R.A., and Kuchroo, V.K. (2015). Tim-1 is essential for induction and maintenance of IL-10 in regulatory B cells and their regulation of tissue inflammation. J. Immunol. *194*, 1602–1608.

Yeung, M.Y., Ding, Q., Brooks, C.R., Xiao, S., Workman, C.J., Vignali, D.A., Ueno, T., Padera, R.F., Kuchroo, V.K., Najafian, N., and Rothstein, D.M. (2015). TIM-1 signaling is required for maintenance and induction of regulatory B cells. Am. J. Transplant. *15*, 942–953.

STAR★METHODS

KEY RESOURCES TABLE

REAGENT or RESOURCE	SOURCE	IDENTIFIER
Antibodies		
Anti-mouse CD19, Clone 6D5	Biolegend	Cat# 115555; RRID: AB_2565970
Anti-mouse B220, Clone RA3-6B	Biolegend	Cat# 103223; RRID: AB_313006
Anti-mouse CD11b, Clone M1/70	Biolegend	Cat# 101257; RRID: AB_2565431
Anti-mouse CD3ε, Clone 145-2C11	Biolegend	Cat# 100320; RRID: AB_312685
Anti-mouse TCRβ, Clone H57-597	Biolegend	Cat# 109230; RRID: AB_2562562
Anti-mouse CD4, Clone RM4-5	Biolegend	Cat# 100543; RRID: AB_10898318
Anti-mouse CD8a, Clone 53-6.7	Biolegend	Cat# 100744; RRID: AB_2562609
Anti-mouse IFN-g, Clone XMG1.2	Biolegend	Cat# 505813; RRID: AB_493312
Anti-mouse IL-17A, Clone TC11-18H10.1	Biolegend	Cat# 506904; RRID: AB_315464
Anti-mouse IL10, Clone JES5-16E3	Biolegend	Cat# 505008; RRID: AB_315362
Anti-mouse TIGIT, Clone 1G9	Biolegend	Cat# 142107; RRID: AB_2565648
Anti-mouse CD62L, Clone MEL-14	Biolegend	Cat:#104406; RRID: AB_313039
Anti-mouse/human CD44, Clone IM7	Biolegend	Cat# 103012; RRID: AB_312963
Anti-mouse CD11c, Clone N418	Biolegend	Cat# 117334; RRID: AB_2562415
Anti-mouse TIM-1, Clone RMT1-4	Biolegend	Cat# 119506; RRID: AB_2232887
Anti-mouse CD45	Biolegend	Cat# 103108; RRID: AB_312973
Anti-mouse CD138, Clone 281-2	Biolegend	Cat# 142506; RRID: AB_10962911
Anti-mouse CD21, Clone CR2/CR1	Biolegend	Cat# 123412; RRID: AB_2085160
Anti-mouse CD23, Clone B3B4	Biolegend	Cat# 101606; RRID: AB_312831
Anti-mouse PD-1, Clone RMP1-30	Biolegend	Cat:#109110; RRID: AB_572017
Anti-mouse LAG-3, Clone C9B7W	Biolegend	Cat# 125212; RRID: AB_2561517
Anti-mouse Tim-3, Clone 5D12	Biolegend	Custom made
Anti-mouse TIM-1, Clone 5F12	Xiao et al., 2015	N/A
Anti-mouse CD93, Clone AA4.1	eBioscience	Cat# 17-5892-82; RRID: AB_469466
Anti-mouse FAS, Clone Jo2	BD Biosciences	Cat# 557653; RRID: AB_396768
Anti-mouse GL-7, Clone GL-7	BD Biosciences	Cat# 562080; RRID: AB_10894953
AffiniPure Fab Fragment Goat Anti-Mouse IgM, μ chain specific	Jackson ImmunoResearch	Cat# 115-007-020; RRID: AB_2338477
Anti-mouse AhR, Clone 4MEJJ	Thermo Fisher Scientific	Cat# 12-5925-82; RRID: AB_2572644
Anti-mouse FoxP3, Clone FJK-16	ThermoFisher Scientific	Cat# 17-5773-82; RRID: AB_469457
Chemicals, Peptides, and Recombinant Proteins		
Lipopolysaccharide (LPS)	Sigma Aldrich	Cat# L4391
Dexamethasone	Sigma Aldrich	Cat# D4902
Phorbol-12-myristate-13 acetate (PMA)	Sigma Aldrich	Cat# P8139
Ionomycin	Sigma Aldrich	Cat# I0634
Complete Freund's adjuvant (CFA)	BD Difco	Cat# 263810
M. tuberculosis H37 Ra, desiccated	BD Difco	Cat# 231141
7AAD	BD Biosciences	Cat# 559925
Golgi Stop	BD Biosciences	Cat# 554724
Fixable Viability w eFluor 506	Invitrogen	Cat# 65-0866-14
MOG_{35-55} peptide	Quality Controlled Biochemicals	N/A
Pertussis toxin	List Biological Laboratories	Cat# 180

(*Continued on next page*)

Continued

REAGENT or RESOURCE	SOURCE	IDENTIFIER
Critical Commercial Assays		
LegendPlex (Mouse Th Cytokine Panel)	Biolegend	Cat# 740005
BD Cytofix/Cytoperm	BD Biosciences	Cat# 51-2090KZ
BD Perm/Wash	BD Biosciences	Cat# 51-2091KZ
CellTrace Violet Cell Proliferation Kit	Invitrogen	Cat# C34557
Fixation/Permeabilization Concentrate	Invitrogen	Cat# 00-5123-43
Fixation/Perm Diluent	Invitrogen	Cat# 00-5223-56
Permeabilization Buffer	Invitrogen	Cat# 00-8333-56
RNeasy Plus Mini Kit	QIAGEN	Cat# 74134
RNase-Free DNase Set	QIAGEN	Cat# 79254
iScript cDNA Synthesis Kit	Bio-Rad	Cat# 1708891
CD19 MicroBeads, mouse	Miltenyi Biotec	Cat# 130-052-201
SuperScript IV VILO Master Mix	Thermo Fisher Scientific	Cat# 11756050
TaqMan Fast Advanced Master Mix	Thermo Fisher Scientific	Cat# 4444557
PicoPure RNA Isolation Kit	Thermo Fisher Scientific	Cat# KIT0204
Deposited Data		
Raw and analyzed data	This paper	GEO: GSE150786
Experimental Models: Organisms/Strains		
Tim-1$^{fl/fl}$ mice	This paper	N/A
Tigit$^{fl/fl}$ mice	This paper	N/A
Tim-1^{BKO} mice	This paper	N/A
Tigit^{BKO} mice	This paper	N/A
Tim-1$^{-/-}$ mice	Xiao et al., 2015	N/A
Tim-1$^{\Delta mucin}$ mice	Xiao et al., 2015	N/A
Tigit$^{-/-}$ mice	Joller et al., 2014	N/A
C57BL/6 mice	Jackson laboratory	Cat# JAX:000664; RRID: IMSR_JAX:000664
CD19^{Cre} mice	The Jackson Laboratory	Cat# JAX:006785; RRID: IMSR_JAX:006785
Rag1$^{-/-}$ mice	The Jackson Laboratory	Cat# JAX:002216; RRID: IMSR_JAX:002216
B6.129P2-Igh-Jtm1Cgn/J mice	The Jackson Laboratory	Cat# 002438; RRID: IMSR_JAX:002438
IL10^{GFP} tiger mice	The Jackson Laboratory	Cat# JAX:008379; RRID: IMSR_JAX:008379
AhR^{d} mice	The Jackson Laboratory	Cat# JAX:002921; RRID: IMSR_JAX:002921
Software and Algorithms		
FlowJo v10.5.0	FlowJo	https://ww.flowjo.com
Prism v7.0a and v8.1.2	GraphPad	https://ww.graphpad.com
R	N/A	https://www.r-project.org/
Other		
anti-CD3/anti-CD28 beads	Invitrogen	Cat# 11456D
DNase I	Sigma-Aldrich	DN25
Collagenase D	Sigma-Aldrich	Cat# 11088882001

RESOURCE AVAILABILITY

Lead Contact

Further information and requests for resources and reagents should be directed to and will be fulfilled by the Lead Contact, Vijay K. Kuchroo.

Email: vkuchroo@evergrande.hms.harvard.edu

Materials Availability

All unique/stable materials generated in this study are available from the lead contact with a completed Material Transfer Agreement.

Data and Code Availability

The accession number for the RNA-seq data reported in this paper is GEO: GSE150786

EXPERIMENTAL MODEL AND SUBJECT DETAILS

Animals

Tim-1 and Tigit floxed mice were generate on the C57BL/6 background. Targeting vectors containing genomic fragments of the Tim-1 or Tigit gene were constructed by using C57BL/6 BAC clones. Linearized targeting vector was transfected into B6 embryonic stem (ES) cells. Homologous recombinants were identified by Southern-blot analysis, and were implanted into foster B6-albino mothers. Chimeric mice were bred to C57BL/6 mice, and the F1 generation was screened for germline transmission. The Neo gene was removed by breeding F1 mice with a strain of actin promoter-driven Flipase transgenic mice (Jackson Laboratory, 003800). C57BL/6 mice (000664), $CD19^{Cre}$ (006785), $IL10^{GFP}$ tiger (008379), AhR^{d} (002921), muMT (002288), and $Rag1^{-/-}$ (002216) mice were purchased from the Jackson Laboratory. Tim-$1^{-/-}$, Tim-$1^{\Delta mucin}$, and $Tigit^{-/-}$ mice, all on the C57BL/6 background, were described previously (Joller et al., 2014; Xiao et al., 2015). Both females and males were used in the study. Ages of mice were indicated in figure legends. Mice were maintained and all animal experiments were done according to the animal protocol guidelines of Harvard Medical School.

METHOD DETAILS

Cell purification and cultures

For AC preparation, thymocytes from C57BL/6 mice were treated with 1 μM dexamethasone (Sigma-Aldrich) for 8h. After an extensive wash, AC were used in cell cultures. Annexin V and propidium iodide (BD Biosciences) staining was used to confirm apoptosis of thymocytes.

Splenic B cells were purified using MACS columns following staining with anti-mouse CD19 MACS beads. Cells were cultured in round-bottom 96-well plates in the presence of anti-Tim-1 (clone 5F12), AC, $(Fab')_2$ fragment anti-IgM, Anti-CD40, IL-21, or their combinations. After 3 days, IL-10 production in culture supernatants was measured by cytokine bead array (CBA) or ELISA. MACS purified $CD19^+$ B cells were labeled with PE-anti-Tim-1 (RMT1-4) and then separated into Tim-1^+ and Tim-1^- B cells by fluorescence-activated cell sorting for further uses.

$CD4^+CD62L^{hi}CD25^-$ naive $CD4^+$ T cells were purified by fluorescence-activated cell sorting after a MACS bead isolation of $CD4^+$ cells as previously described (Xiao et al., 2015). Naive $CD4^+$ cells were activated with isolated $CD19^+$ B cells plus soluble anti-CD3 (1 μg/ml). After 96 h, cells were collected for further experiments.

Single-cell suspensions from colon lamina propria tissue were prepared using the Lamina Propria Dissociation Kit (Miltenyi Biotec). Isolated cells were resuspended in culture medium for further analysis. For isolation of CNS-infiltrating mononuclear cells, mice were first perfused through the left cardiac ventricle with cold PBS. The forebrain and cerebellum were dissected and spinal cords flushed out with PBS by hydrostatic pressure. CNS tissue was cut into pieces and digested with collagenase D (2.5 mg/ml, Roche Diagnostics) and DNase I (1 mg/ml, Sigma) at 37°C for 30 min. Mononuclear cells were isolated by passing the tissue through a 70 μm cell strainer, followed by a 70%/37% percoll gradient centrifugation. Mononuclear cells were removed from the interphase, washed, and resuspended in culture medium for further analysis.

For *in vitro* suppression assay, 5×10^4 FACS-sorted $CD3e^+$ $CD4^+$ $CD25^-$ conventional T cells (Tconv) from LNs and spleens of $CD19^{Cre/WT}$ mice were labeled with 5 μM CellTrace Violet and stimulated with anti-CD3/anti-CD28 beads(Dynabeads, Invitrogen) in presence of FACS sorted $CD3e^+$ $CD4^+$ $CD25^+$ Treg cells from $CD19^{Cre/WT}$, TIM-1^{BKO} or $TIGIT^{BKO}$ mice. Tconv proliferation was read out after 72h by flow cytometry and the division index of responder cells was analyzed using FlowJo based on the division of Cell Trace Violet. Suppression was then calculated with the formula % Suppression = (1-DivTreg/DivAlone) x100% (DivTreg stands for the division index of responder cells with Tregs, and DivAlone stands for the division index of responder cells activated without Tregs).

Flow cytometry

For intracellular cytokine staining, cells were stimulated in culture medium containing phorbol 12-myristate 13-acetate (30 ng/ml, Sigma-Aldrich), ionomycin (500 ng/ml, Sigma-Aldrich), and GolgiStop (1 μl/ml, BD Biosciences) in a cell incubator with 10% CO_2 at 37°C for 4 h. After surface markers were stained, cells were fixed and permeabilized with Cytofix/Cytoperm and Perm/Wash buffer (BD Biosciences) according to the manufacturer's instructions. Then, cells were stained with fluorescence-conjugated cytokine antibodies at RT for 30 min before analysis. 7-AAD (BD Biosciences) was also included to gate out the dead cells. All data were collected on a FACSCalibur or an LSR II (BD Biosciences) and analyzed with FlowJo software (TreeStar).

EAE

Mice were immunized subcutaneously in the flanks with an emulsion containing MOG_{35-55} (80 μg/mouse) and *M. tuberculosis* H37Ra extract (3 mg/ml, Difco Laboratories) in CFA (100 μl/mouse). Pertussis toxin (100 ng/mouse, List Biological Laboratories) was administered intraperitoneally on days 0 and 2. Mice were monitored and assigned grades for clinical signs of EAE as previously described

(Xiao et al., 2015). To evaluate the suppressive ability of Tim-1$^+$ B cells, purified total B cells or Tim-1$^+$ B cells were transferred i.v. into WT recipients. Hosts were then immunized to induce EAE.

Chromatin immunoprecipitation (ChIP)

B cells from WT and AhR^d mice were treated for 24 h with anti-Tim-1 or control rIgG1, fixed with 1% formaldehyde for 15 min, and quenched with 0.125 M glycine. Chromatin was isolated and sheared to an average length of 300–500 bp by sonication. Genomic DNA (Input) was prepared by treating aliquots of chromatin with RNase, proteinase K and heated for de-crosslinking, followed by ethanol precipitation. AhR-bound DNA sequences were immuno-precipitated with an AhR-specific antibody (Biomol SA-210). Crosslinks were reversed by incubation overnight at 65 C, and ChIP DNA was purified by phenol-chloroform extraction and ethanol precipitation. Quantitative PCR (qPCR) reactions were carried out in triplicate and experimental C_t values were converted to copy numbers detected by comparison with a DNA standard curve run on the same PCR plates. Copy number values were normalized for primer efficiency using the values obtained with input DNA and the same primer pairs.

RNA isolation, real-time PCR, and histology

RNA was extracted with RNeasy Plus kits (QIAGEN) and cDNA was made using iScript (BioRad). All of the real-time PCR probes were purchased from Applied Biosystems. Quantitative PCRs were performed using ViiA 7 Real-Time PCR System (Applied Biosystems).

Tissues and organs from mice were fixed in 10% neutral buffered formalin for > 12 h, processed, embedded in paraffin wax, sectioned, and stained with H&E using standard procedures. Evaluations were made in a blinded fashion.

RNA-seq assay

Samples from isolated Tim-1$^-$ and Tim-1$^+$ B cells were processed with the SMART-Seq2 protocol (Picelli et al., 2013), and sequenced on Illumina Hi-Seq 2500. The paired-end 38bp reads sequenced (26.53M ± 1.62M pairs of reads per sample) for each of the 8 samples (4 Tim-1$^+$ and 4 Tim-1$^-$ B cell samples derived from naive WT mice) were aligned to the mouse mm10 UCSC reference genome using Tophat version 2.0.10 (Kim et al., 2013) with default settings (read alignment rate of 82.81% ± 0.44% properly mapped pairs per sample). Gene expression levels were quantified for 22,815 genes in the mouse mm10 UCSC reference gene annotations using Cuffquant in the Cufflinks suite version 2.2.1 (Trapnell et al., 2012). These levels were subsequently normalized across all 8 samples using Cuffnorm with default settings based on ''geometric'' normalization, which normalizes samples based on the median expression level in each sample, thus reporting normalized expression levels (FPKM: fragments per kilo bases of exons for per million mapped reads). Out of the 22,815 quantified reference genes, 15,519 genes were detected in at least one of the 8 samples at a normalized FPKM level > 0. Differential gene expression analysis comparing the 4 Tim-1$^+$ and 4 Tim-1$^-$ B cell samples was performed by estimating the asymptotic t test (Student's t-distribution) p values, False Discovery Rate (FDR) (Benjamini and Hochberg) values and fold-changes using the ComparativeMarkerSelection module in GenePattern (Reich et al., 2006). Significantly differentially expressed genes were identified using the asymptotic t test p value $\leq$ 0.05 and absolute fold change $\geq$ 2 selection criteria. Heatmaps visualizing the normalized gene expression levels (zero mean centering and unit standard deviation scaling of the expression levels for each gene, followed by saturating these normalized gene expression levels at +1 and −1) were generated using GENE-E/Morpheus.

QUANTIFICATION AND STATISTICAL ANALYSIS

The clinical score and incidence of EAE were analyzed by Fisher's exact test (Figures 3A, 4C, S4F, and S5B), and comparisons for results (mean ± SEM) of BioLegend LEGENDplex (Figures 1D and 1E), ELISA (Figures 1C, 4B, and S4C), FACS (Figures 2C, 2E, 3B, 4F, S1C–S1F, S4D, S5D–S5F, and S5H–S5J), and real-time PCR (Figures 3F, S4B, and S4E) were analyzed by Student's t test. $p < 0.05$ was considered significant. Significantly differentially expressed genes for RNA-seq analysis were identified using the asymptotic t test p value $\leq$ 0.05 (Figures 3C–3E and S4A).